Hybrid Epoxy Systems Modified with *Abies alba* Exudate: Cotton *versus* Silk Reinforcements

Cosmin Mihai Mirițoiu,[a,*] Dragoș Tutunea,[b,*] Silvia Ștefania Nedelcu Văduva,[a] and Adrian Giura [b]

The mechanical behavior of hybrid composite materials was studied based on a matrix composed of 50 wt.% *Abies alba* exudate and 50 wt.% epoxy resin, reinforced with cotton and silk fabrics. Composite plates were manufactured using a hand lay-up technique with a 40/60 resin-to-reinforcement ratio. Mechanical characterization included tensile, flexural, vibration, and Shore D hardness tests, supported by statistical analysis using one-way ANOVA and Bonferroni post hoc comparisons. The results showed that the introduction of textile reinforcement significantly improved all investigated properties compared to the unreinforced hybrid resin. Cotton-reinforced composites exhibited the highest tensile and flexural strength, as well as the highest hardness values, indicating increased stiffness and load-bearing capacity. In contrast, silk-reinforced composites demonstrated superior deformation capacity and higher damping behavior, reflecting enhanced ductility and energy dissipation. Statistical analysis confirmed a highly significant influence of material configuration on all properties ($p < 0.05$). An exception was observed in flexural deformation, where no significant difference was found between cotton- and silk-reinforced composites, suggesting a similar global deformation response. The results demonstrate that hybrid epoxy systems modified with *Abies alba* exudate can be successfully used for the development of bio-based composites.

DOI: 10.15376/biores.21.4.10032-10048

Keywords: Abies alba exudate; Cotton fabric; Silk fabric; Mechanical properties

Contact information: a: University of Craiova, Faculty of Mechanics, Department of Applied Mechanics and Civil Constructions, Craiova, Romania; b: University of Craiova, Faculty of Mechanics, Department of Vehicles, Transports and Industrial Engineering, Craiova, Romania;
** Corresponding author: miritoiucosmin@yahoo.com, dragostutunea@yahoo.com*

INTRODUCTION

The growing emphasis on sustainability has stimulated increasing interest in bio-derived materials, particularly bio-based polymers and natural resin systems, as viable substitutes for conventional petroleum-based matrices. Natural resins such as rosin, dammar, sandarac, manila copal, mastic, or shellac have been widely explored owing to their renewable nature and their potential for use in eco-friendly composite applications. Nevertheless, the direct application of natural resins as structural matrices is often constrained by their relatively modest mechanical properties and processing limitations. To address these drawbacks, hybrid formulations incorporating natural resins into synthetic polymer systems, especially epoxy resins, have been proposed.

In this context, attention has gradually turned to specific natural resins that can be incorporated into epoxy systems, with each type of resin offering particular advantages and limitations, depending on its chemical nature and compatibility with the synthetic matrix. Among these, dammar resin has attracted particular interest as a natural component in epoxy-based hybrid systems. Franz *et al.* (2021) investigated hybrid composites obtained by formulating natural dammar resin with epoxy resin, using dammar volume fractions of 60%, 70%, and 80%. Their study examined both the chemical characteristics of the resin system and the mechanical behavior of the resulting hybrid composites. It was shown that no new chemical bonds were formed between dammar resin and epoxy resin, while curing took place only through the reaction between the epoxy resin and its hardener. Bolcu *et al.* (2022) studied wheat straw-reinforced composites with Dammar-based hybrid matrices containing 50% and 70% natural resin. Their results indicated that the incorporation of Dammar improved damping behavior, although it also reduced the mechanical strength of the resulting composites.

Shellac has also been investigated in combination with epoxy resins. For example, Goswami and Kumar (1984) studied the curing behavior of shellac–epoxy blends by dielectric measurements and showed that the hardening process developed mainly during the first days after mixing, followed by a gradual stabilization of the electrical properties of the system. In another approach, shellac was blended with an epoxidised novolac resin to improve its performance as a coating material (Ansari *et al.* 2014). The study suggested that the presence of the synthetic component made the natural resin more suitable for practical use by enhancing its overall behavior. Such results show that natural resins can be successfully upgraded through incorporation into synthetic resin systems.

In another approach, natural lacquer (urushi) was combined with a bisphenol A-type epoxy resin and organosilane compounds to develop a bio-based hybrid resin. The study Kanehashi *et al.* (2014) showed that the hybridization process improved drying, hardness, and molding behavior, suggesting that natural resin systems can be successfully integrated into synthetic networks for more demanding applications. Natural lacquer (urushi) has also been explored in hybrid resin systems. Earlier studies, such as Takahisa *et al.* (2006), examined the reaction between urushiol and organosilane compounds, showing that such hybridization can accelerate curing and improve film properties. In a further development, natural lacquer was combined with a bisphenol A-type epoxy resin and organosilanes to obtain a bio-based hybrid resin with improved drying, hardness, and molding behavior.

Rosin has been explored more extensively than many other natural resins in relation to epoxy systems, and its derivatives have been used both as epoxy precursors and as curing components in bio-based thermosetting formulations. In Deng *et al.* (2023), rosin-based epoxy monomers with different flexible chain lengths were synthesized and cured with several amine curing agents in order to evaluate their adhesion, toughness, hardness, water resistance, heat resistance, and weatherability. The results showed that introducing an appropriate flexible chain into the rosin-based epoxy monomer improved toughness and adhesion, while the rosin-based resins also exhibited better adhesion and weather resistance than a commercial bisphenol A epoxy resin. Brocas *et al.* (2014) prepared epoxy resins using epoxidized rosin acids as co-precursors together with DGEBA (diglycidyl ether of bisphenol A), showing that rosin-derived structures can be directly incorporated into epoxy networks. Their results suggested that renewable rosin can serve as a viable building block for partially bio-based epoxy formulations. In El-Ghazawy *et al.* (2015), a fully rosin-based epoxy coating was synthesized and structurally characterized by spectroscopic methods. The work showed that rosin-derived epoxy systems can provide thermal and mechanical performance comparable to, or in some respects better than, conventional bisphenol A-based systems. Li *et al.* (2013) synthesized a rosin-based epoxy monomer and compared it with a petroleum-based counterpart. The study highlighted the potential of rosin as a renewable precursor for epoxy materials intended to replace conventional petrochemical components. Liu *et al.* (2022) used maleopimaric acid, a rosin-derived compound, in a bisphenol A epoxy curing system and examined its curing behavior and final properties. They found that the rosin-based component increased rigidity and thermal resistance, although it also made the system more brittle. Huang *et al.* (2013) combined a rigid rosin-based epoxy with a more flexible dimer-acid-based epoxy in order to balance mechanical and thermal performance. Their results showed that the two bio-based epoxy components could complement each other and produce systems with improved overall properties.

Sandarac has also been considered in hybrid resin formulations for green composites. In Mirițoiu *et al.* (2021), hybrid systems based on sandarac and epoxy were used together with natural textile reinforcements, and the results showed that such materials can be processed into sandwich-type composites, although their mechanical performance remained lower than that of comparable dammar-based systems.

Taken together, these studies show that several natural resins can be successfully incorporated into synthetic resin systems, particularly epoxy-based ones, in order to obtain hybrid materials with improved functional performance. Within this context, *Abies alba* exudate emerges as an interesting and still insufficiently explored natural resin for the development of hybrid composite matrices. Therefore, the present work examines the use of *Abies alba* exudate as a natural component in hybrid epoxy matrices for composites reinforced with cotton and silk fabrics, with particular attention to the way in which the reinforcement type affects the mechanical response of the material.

EXPERIMENTAL

Materials and Methods

This study investigated the use of fir resin (*Abies alba* exudate) as a natural component in a hybrid matrix intended for composite materials. The resin was collected free of charge from the Baia de Fier village, Gorj County, Romania. Naturally, the resin appears on the surface of fir trees, where, upon exposure to air, it undergoes oxidation and the volatile compounds gradually evaporate. As a result, it transforms into a hardened, stone-like material, which in this state cannot be directly used as a component in hybrid resin systems. To enable its utilization, the resin was first dissolved in a suitable solvent, such as turpentine obtained from pine buds, as illustrated in Fig. 1. For dissolution, the *Abies alba* exudate and turpentine were mixed at a 1:1 mass ratio, corresponding to 50 wt% exudate and 50 wt% turpentine. Both components were weighed individually, placed in sealed containers, and maintained under closed conditions throughout the dissolution process. Once liquefied, it was blended with a synthetic resin to form a hybrid matrix (Fig. 2). The synthetic component consisted of Resoltech 1050 epoxy resin combined with its corresponding 1055 hardener. The synthetic epoxy resin was purchased from a local supplier (see Polydis (2023)). The addition of the synthetic resin is essential to ensure proper polymerization and the formation of a solid material. The *Abies alba* exudate, once dissolved in solvent, does not undergo curing or solidification on its own. In this form, it cannot be used independently as a matrix material, which justifies its incorporation into a hybrid resin system.

For the unreinforced material, the *Abies alba* exudate, Resoltech 1050 epoxy resin, and Resoltech 1055 hardener were mixed for 3 min at room temperature (approximately 20 °C) to obtain a homogeneous mixture. After mixing, the resulting material was poured into the mold, where polymerization continued.

All investigated materials were cured at room temperature and demolded after 7 days. From the final polymerized plate obtained by combining *Abies alba* exudate with the synthetic resin, specimens were cut and prepared for the tests presented in this study. An example consisting of five specimens extracted from the final plate is illustrated in Fig. 2. Furthermore, the term hybrid, as used in the present work, refers to a physically blended and polymerized system rather than a chemically bonded one, since it has already been demonstrated that no new chemical reactions occur between the *Abies alba* exudate and the epoxy-based synthetic resin (Miriţoiu *et al.* 2026).

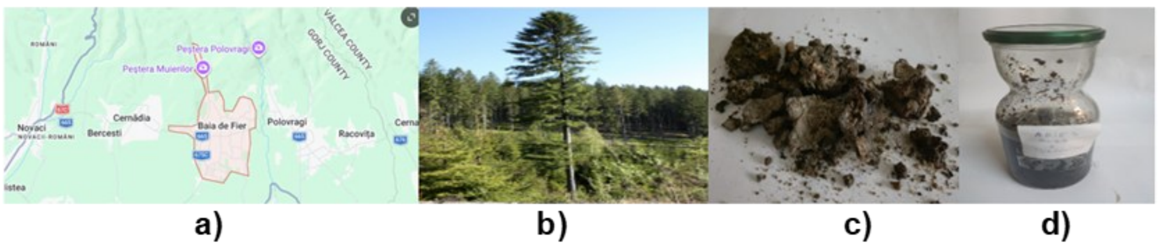

Fig. 1. Main stages of *Abies alba* exudate collection and preparation: (a) field sampling location; (b) natural exudation environment; (c) raw Abies alba exudate; and (d) dissolution in turpentine at an exudate-to-turpentine mass ratio of 1:1

Fig. 2. Schematic representation of the process of combining natural and synthetic resins to obtain a solid material, along with the highlighting of specimens cut from the hybrid resin plate

To demonstrate the applicability of the hybrid resin, composite materials reinforced with cotton and silk fibers were fabricated, using the hybrid matrix based on *Abies alba* exudate. A mass ratio of 40% resin and 60% reinforcement was employed. The hybrid resin composition consisted of 50 wt.% *Abies alba* exudate and 50 wt.% synthetic epoxy resin. Both fibers were purchased from local suppliers. The cotton reinforcement consisted of a plain-woven fabric with an areal weight of 130 g/m^2, whereas the silk reinforcement consisted of a 100% silk taffeta fabric with a plain-weave structure and an areal weight of 105 g/m^2. A general view of a plate fabricated by casting using the hand lay-up technique is presented in Fig. 3, while Figs. 4 and 5 illustrate representative specimens made of silk and cotton, respectively. During fabrication, the resin was applied over the first reinforcement layer, followed by the placement of a second reinforcement layer, over which resin was again applied. This procedure was repeated for a total of 12 layers.

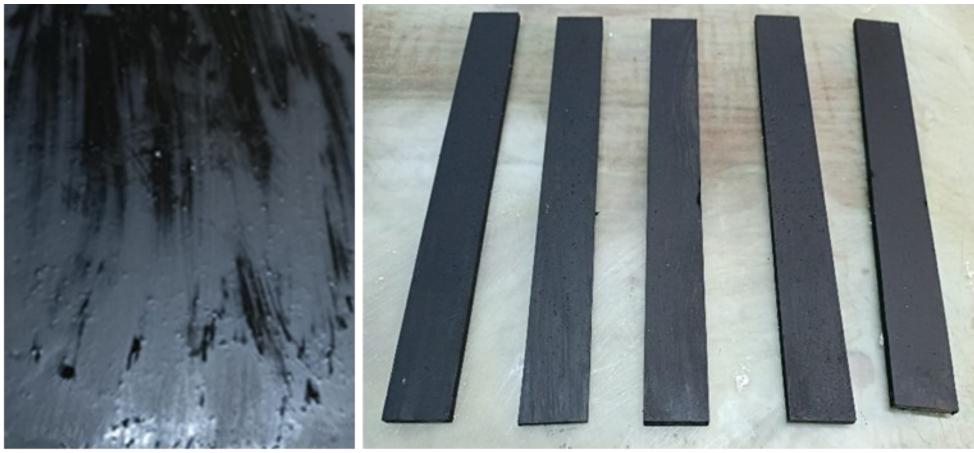

Fig. 3. (a) A general view of the hybrid resin composite plate reinforced with silk fibers; (b) Specimens reinforced with silk fiber, cut from the cast plate and used for tensile testing

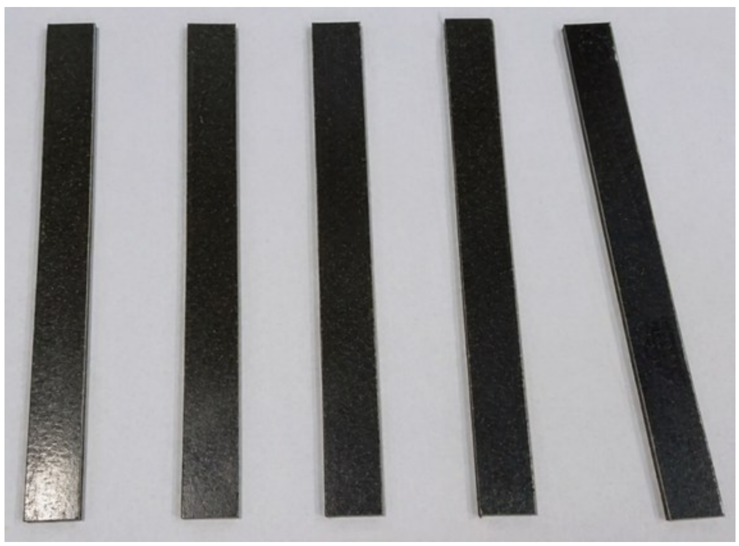

Fig. 4. Specimens reinforced with cotton fiber, cut from the cast plate and used for tensile testing

Test Standards and Characterizations

Tensile test

For the tensile characterization, plates were first produced exclusively from the hybrid resin system composed of 50 wt.% *Abies alba* exudate and 50 wt.% Resoltech 1050 epoxy resin with 1055 hardener (Fig. 2). In a subsequent stage, composite laminates were manufactured by incorporating cotton and silk fibers as reinforcement phases, while maintaining the same hybrid resin as the matrix material (Figs. 3 and 4). A set of 10 specimens was prepared from each plate. The samples were designated as AA for the unreinforced hybrid resin, AAC for the cotton fiber-reinforced composites, and AAS for the silk fiber-reinforced composites. Tensile testing was conducted in accordance with ASTM D3039/D3039M-08 (2014), using specimens with dimensions of 250 mm in length, 25 mm in width, and 8 mm in thickness. The experiments were performed on a Laryee (Beijing, China) universal testing machine equipped with a 10 kN load cell. The tensile tests were performed at a constant crosshead displacement rate of 2 mm/min.

Bending test

Flexural testing was carried out on plates prepared in a manner analogous to those used in tensile investigations. Initially, plates consisting solely of the hybrid resin were produced, followed by the fabrication of two additional groups of composite plates reinforced with cotton and silk fibers, respectively. All specimens retained the same 12-layer lay-up configuration adopted in the tensile study. A total of 10 samples were sectioned from each plate, with dimensions of 250 mm in length, 20 mm in width, and 8 mm in thickness. The bending tests were conducted using a Laryee (Beijing, China) universal testing machine fitted with a three-point bending setup. All measurements were performed in accordance with ASTM D790-17 (2017). The span length was set to 128 mm, corresponding to a span-to-thickness ratio of 16:1, in accordance with ASTM D790 requirements. The three-point flexural tests were performed at a constant crosshead displacement rate of 3 mm/min. The samples were designated as AA for the unreinforced hybrid resin, AAC for the cotton fiber-reinforced composites, and AAS for the silk fiber-reinforced composites.

Vibration test

For the vibration analysis, the specimens maintained the same geometry and properties as those employed in the tensile tests. Each specimen was fixed at one end, creating a cantilever configuration, while the free end was instrumented with a Brüel & Kjær accelerometer (sensitivity: 0.04 pC/ms^2). The sensor was connected to a Nexus signal conditioner, which enabled the transmission of the measured signals to a SPIDER 8 data acquisition system (HBK Hottinger Brüel & Kjær, Darmstadt, Germany). The acquisition unit was interfaced with a laptop, where all experimental data were recorded and stored. The samples were designated as AA for the unreinforced hybrid resin, AAC for the cotton fiber-reinforced composites, and AAS for the silk fiber-reinforced composites. A force was applied at the free end of each cantilever specimen, producing an initial bending deformation. The force was then removed at $t=0$, and the specimen was allowed to vibrate freely until the oscillations were damped.

Shore D hardness test

Shore D hardness measurements were carried out in accordance with ASTM D2240-15 (2021). The test specimens had identical dimensions to those used in the tensile experiments. A total of five indentation readings were performed along the longitudinal direction of each specimen. The first and last measurements were positioned at a distance of 25 mm from the specimen edges. To maintain consistency, all readings were taken along the central line of the specimen width. The samples were designated as AA for the unreinforced hybrid resin, AAC for the cotton fiber-reinforced composites, and AAS for the silk fiber-reinforced composites.

Statistical Interpretation of Experimental Data

A statistical analysis was performed. The specimens made exclusively from hybrid resin (AA) were considered as the control group. The analysis was conducted to evaluate whether the type of reinforcement (cotton or silk) had a significant influence on the mechanical properties of the composites. In the initial phase, a statistical power analysis was carried out to verify whether the sample size was sufficient to support reliable conclusions. The experimental datasets were then screened for the presence of outliers, and no anomalous values were identified. Subsequently, the results were evaluated using a one-way ANOVA approach. Both the null and alternative hypotheses were defined, and the decision to reject or retain the null hypothesis was based on the obtained results. To minimize the risk of Type I errors, the assumptions required for ANOVA were also verified, including the normal distribution of data within each group and the homogeneity of variances (Popa *et al.* 2024). As the one-way ANOVA provides an overall comparison among groups, a post hoc analysis with Bonferroni adjustment was conducted to perform pairwise comparisons and identify statistically significant differences between the experimental groups (Obădan *et al.* 2023). All statistical computations were carried out using Microsoft Excel (Microsoft Corp., Redmond, WA, USA). The mathematical models of the statistical methods were consistent with the methodology presented in Mirițoiu *et al.* (2026).

RESULTS AND DISCUSSION

Tensile Test

In the tensile tests, a total of ten specimens were prepared from each plate manufactured using the unreinforced hybrid resin (samples AA), as well as ten specimens from each of the plates reinforced with cotton (samples AAC) and silk fibers (samples AAS). The measured values of tensile strength at failure and extension at break corresponding to all specimens in each material group are illustrated in Figs. 5 and 6.

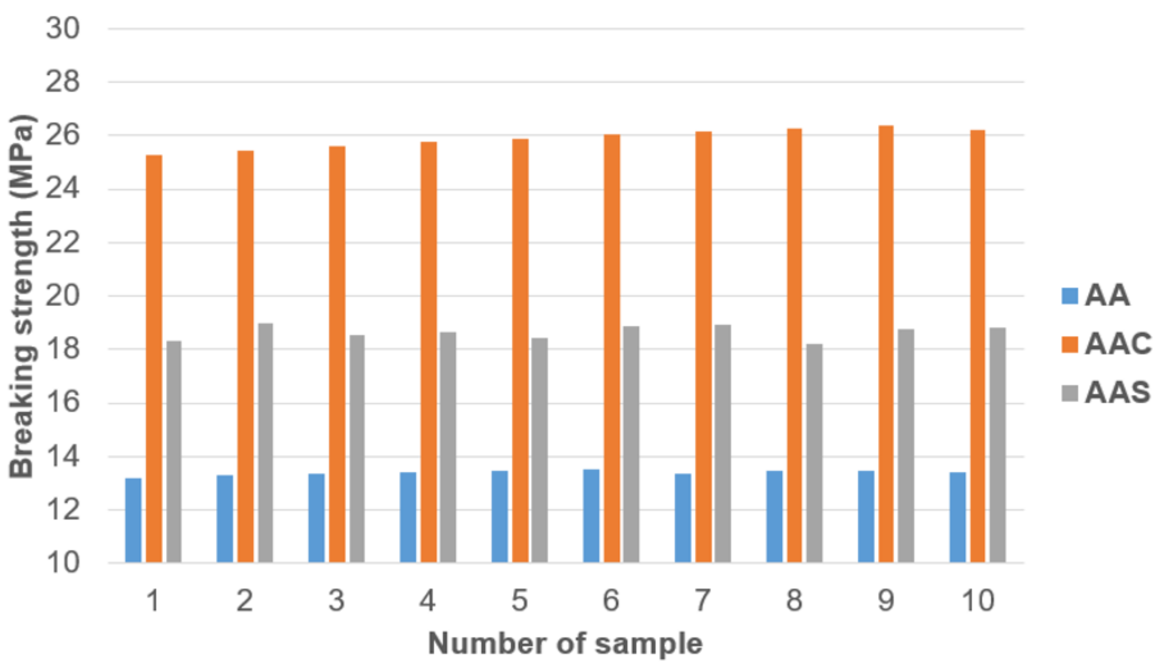

Fig. 5. Tensile strength at failure for the 10 specimens corresponding to each material group

The tensile test results indicate a clear increase in both strength and deformation capacity when reinforcement was introduced. The specimens made only from the hybrid *Abies alba*/epoxy matrix (AA) exhibited the lowest values, while the reinforced materials showed improved performance. The cotton-reinforced composites (AAC) provided the highest tensile strength, whereas the silk-reinforced specimens (AAS) displayed the largest elongation at break. These results suggest that cotton reinforcement favored strength improvement, while silk reinforcement enhanced the deformation capacity of the material. This behavior can be attributed, at least in part, to the different mechanical characteristics of the reinforcing fibers. Cotton fibers tend to exhibit higher stiffness, which contributes to increased strength, whereas silk fibers are capable of sustaining larger strains, leading to improved deformation capacity.

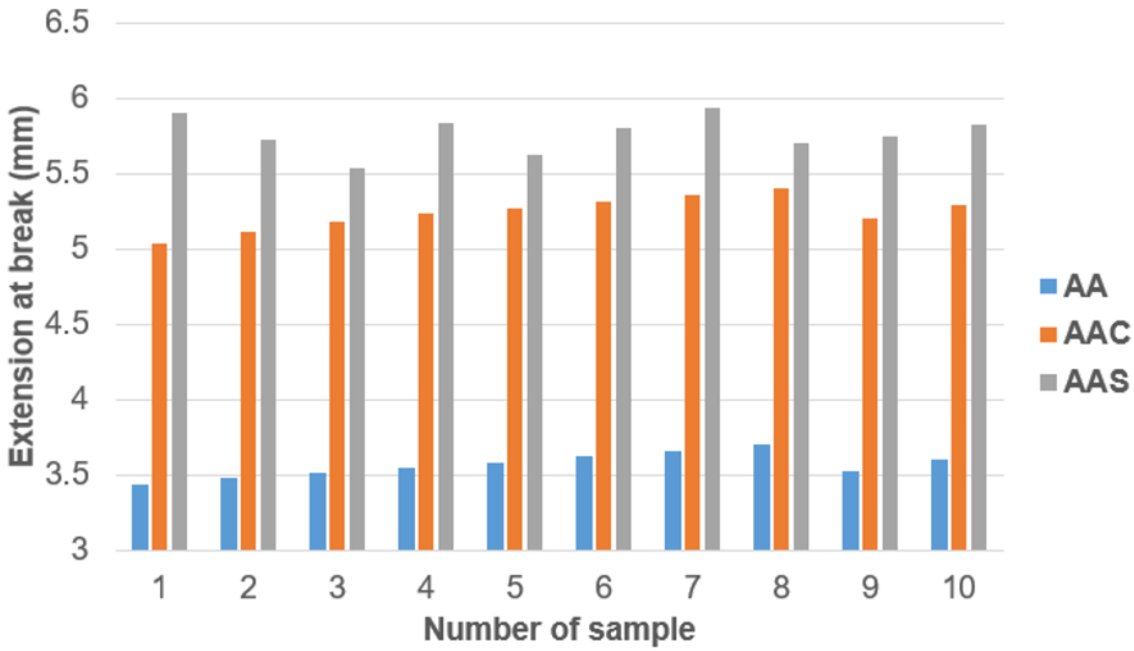

Fig. 6. Extension at break measured for 10 specimens from each material group

A statistical power evaluation was carried out for both the tensile strength data and the extension at break measurements. The statistical power was found to exceed 0.9999, indicating an extremely high sensitivity of the analysis to detect differences between the investigated groups. The values presented in Table 1 indicate that the differences observed in breaking strength among the materials formulations are statistically reliable, and that the selected number of specimens is sufficient for the experimental framework. A similar interpretation can be drawn from the power analysis conducted on the extension at break data.

Table 1. Power Analysis Applied to Tensile Data

Mechanical parameter	Coehn's effect	Power statistics	Conclusion
Breaking strength	19.974477	0.9999999999	a sample size of 10 specimens per group ensures strong reliability of the results
Extension at break	9.2676	0.9999999999	a sample size of 10 specimens per group ensures strong reliability of the results

The Dixon Q test was applied to all datasets in order to identify potential outliers. For all cases, the calculated Q values were below the critical threshold (Q_{critic} = 0.466, α=0.05), indicating that no statistically significant outliers were detected.

In the following stage, a one-way ANOVA analysis was performed, first for tensile strength and then for extension at break. For both properties, the statistical hypotheses were formulated as follows: the null hypothesis (H_0) assumes that there are no significant differences between the group means (AA, AAC, and AAS), while the alternative hypothesis (H_1) states that at least one group mean differs, indicating that the type of material configuration (unreinforced or reinforced with different fibers) significantly influences the tensile mechanical properties. The results of the one-way ANOVA analyses are presented in Table 2.

Table 2. One-Way ANOVA Results for Tensile Properties

Mechanical parameter	SS_B	SS_W	F-value	p-value
Breaking strength	789.377	1.978	5386.23	$1.3 \cdot 10^{-16}$
Extension at break	26.309	0.306	1159.5	$1.6 \cdot 10^{-16}$
Conclusion: for both tensile strength and extension at break, the material configuration (AA, AAC, and AAS) had a statistically significant influence on the investigated mechanical properties. The results indicate that the presence and type of reinforcement led to pronounced differences in mechanical performance.				

To prevent potential bias in the ANOVA analysis, the assumptions of variance homogeneity and normality of the experimental data were examined using Levene's test and the Shapiro–Wilk test, respectively. For Levene's test applied to both tensile strength and extension at break, the hypotheses were defined as follows: the null hypothesis (H_0) states that the group variances are equal, while the alternative hypothesis (H_1) assumes that at least one group exhibits a different variance. For the Shapiro–Wilk test, also performed for tensile strength and extension at break, the null hypothesis (H_0) assumes that the data follow a normal distribution, whereas the alternative hypothesis (H_1) indicates that the data deviate from normality. The outcomes of these tests are summarized in Table 3 for Levene's test and in Table 4 for the Shapiro–Wilk test.

Table 3. Levene Test Results for Tensile Properties

Mechanical parameter	SS_B	SS_W	F-value	p-value
Breaking strength	0.3005	0.5597	7.248	0.0030
Extension at break	0.00536	0.09697	0.746	0.4837
Conclusion: the null hypothesis was rejected for tensile strength ($p < 0.05$), indicating that the variances are not homogeneous, while for extension at break the null hypothesis was not rejected ($p > 0.05$), suggesting that the assumption of homogeneity of variances is satisfied.				

Table 4. Shapiro-Wilk Test Results for Tensile Properties

Breaking strength			
Material	AA	AAC	AAS
p-value	0.384	0.686	0.687
Extension at break			
Material	AA	AAC	AAS
p-value	0.997	0.972	0.957
Conclusion: all p-values are greater than 0.05; therefore, for each group, the null hypothesis of the Shapiro–Wilk test is not rejected, indicating that the data can be considered normally distributed.			

Because Levene's test indicated unequal variances for tensile strength, Welch's ANOVA was additionally considered for this parameter. The outcomes of this test are summarized in Table 5.

Table 5. Welch ANOVA Test Results for Tensile Properties

Mechanical parameter	df_1	df_2	F-value	p-value
Breaking strength	2	13.79	6300.14	$1.11 \cdot 10^{-16}$
Conclusion: The results confirmed a highly significant effect of the material configuration on tensile strength ($p < 0.05$), supporting the conclusions obtained from the standard ANOVA.				

The assumptions required for ANOVA were partially satisfied. The normality of the data was confirmed for both tensile strength and extension at break, while the homogeneity of variances was verified only for extension at break. For tensile strength, the Levene's test indicated unequal variances; therefore, Welch's ANOVA was additionally considered. To further investigate the differences between the material configurations (AA, AAC, and AAS), a post hoc analysis with Bonferroni correction was performed. Pairwise comparisons were conducted between AA and AAC, AA and AAS, and AAC and AAS. A significance level of $\alpha = 0.0167$ was adopted. The results are presented in Table 6.

Table 6. ANOVA Post Hoc Results with Bonferroni Correction for Tensile Properties

Pair	AA vs AAS	AA vs AAC	AAS vs AAC
p-value (breaking strength)	$1.2 \cdot 10^{-28}$	$3.6 \cdot 10^{-26}$	$2.4 \cdot 10^{-11}$
Pair	AA vs AAS	AA vs AAC	AAS vs AAC
p-value (elongation at break)	$4.1 \cdot 10^{-18}$	$5.8 \cdot 10^{-18}$	$3.01 \cdot 10^{-7}$
Conclusion: The Bonferroni-adjusted post hoc analysis for elongation at break revealed statistically significant differences between all material pairs. Although the difference between AAC and AAS was less pronounced compared to the other comparisons, it remained statistically significant ($p< 0.0167$).			

The statistical analysis demonstrates that the material configuration (AA, AAC, and AAS) has a significant effect on both tensile strength and extension at break, with all groups showing statistically distinct behavior.

Bending Test

During the flexural tests, the experimental procedure followed a similar approach to that used in the tensile investigations. The obtained results are illustrated in Figs. 7 and 8. A behavior consistent with the tensile analysis was observed. The bending results showed that the introduction of reinforcement led to a clear improvement in mechanical performance, with the AAC specimens exhibiting higher flexural strength, while the AAS specimens demonstrated increased deformation capacity. These trends indicate that the type of reinforcement influenced the balance between strength and ductility, and the observed differences were subsequently confirmed through statistical analysis.

A statistical power analysis confirmed that the use of 10 specimens per group ensured highly reliable results for both flexural strength and deformation (power ≈ 1). No outliers were identified in the datasets, as indicated by the Dixon test ($\alpha = 0.05$). The one-way ANOVA revealed a highly significant effect of the material configuration (AA, AAC, and AAS) on flexural strength ($F = 9363.2$, $p < 0.0001$) and deformation ($F = 751.1$, $p < 0.0001$). Levene's test ($p = 0.121$ for strength and $p = 0.094$ for deformation) confirmed the homogeneity of variances, while the Shapiro–Wilk test ($p > 0.05$ for all groups, breaking strength: for AA p= 0.9100, for AAS p= 0.5127, for AAC p= 0.8024; deformation: for AA p= 0.6498, for AAS p= 0.7362, for AAC p= 0.7322) indicated that the data followed a normal distribution. Post hoc comparisons using Bonferroni correction

(α = 0.0167) showed statistically significant differences between all material pairs for flexural strength. For deformation, statistically significant differences were observed between AA and AAC, as well as between AA and AAS. However, no statistically significant difference was found between AAC and AAS ($p = 0.023 > 0.0167$), indicating a similar deformation behavior of the two reinforced composites. For breaking strength, the p-values were $1.2 \cdot 10^{-28}$ (AA vs AAC), $3.6 \cdot 10^{-26}$ (AA vs AAS), and $2.4 \cdot 10^{-27}$ (AAC vs AAS). For the deformation, the corresponding adjusted p-values were $4.1 \cdot 10^{-18}$ (AA vs AAC), $5.80 \cdot 10^{-18}$(AA vs AAS), and 0.023 (AAS vs AAC).

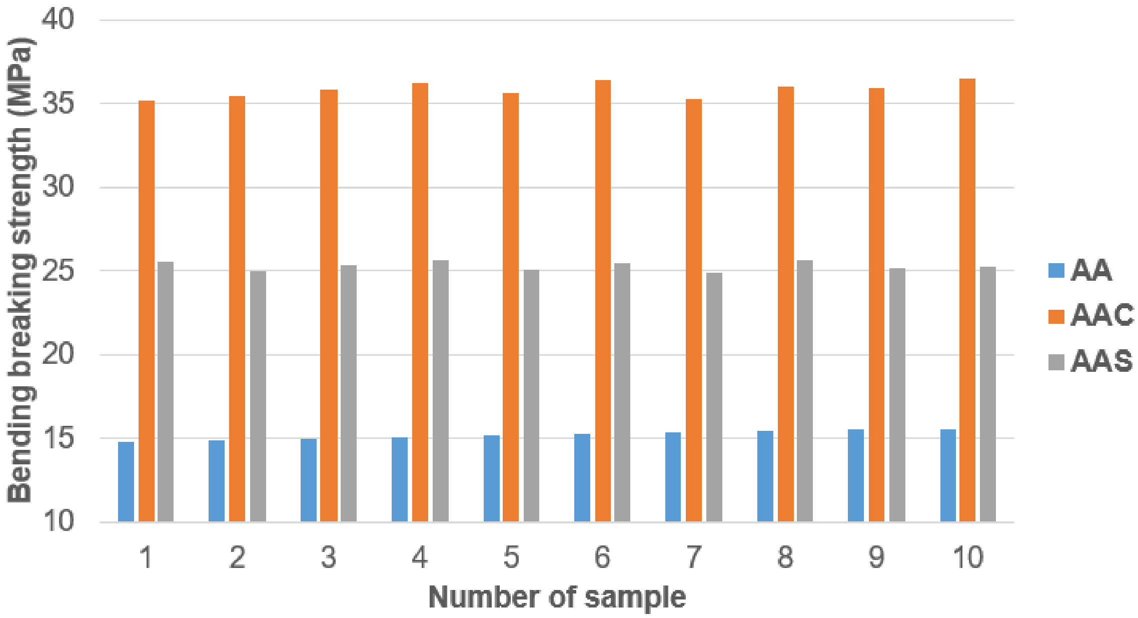

Fig. 7. Flexural strength at failure measured for 10 specimens in each material group

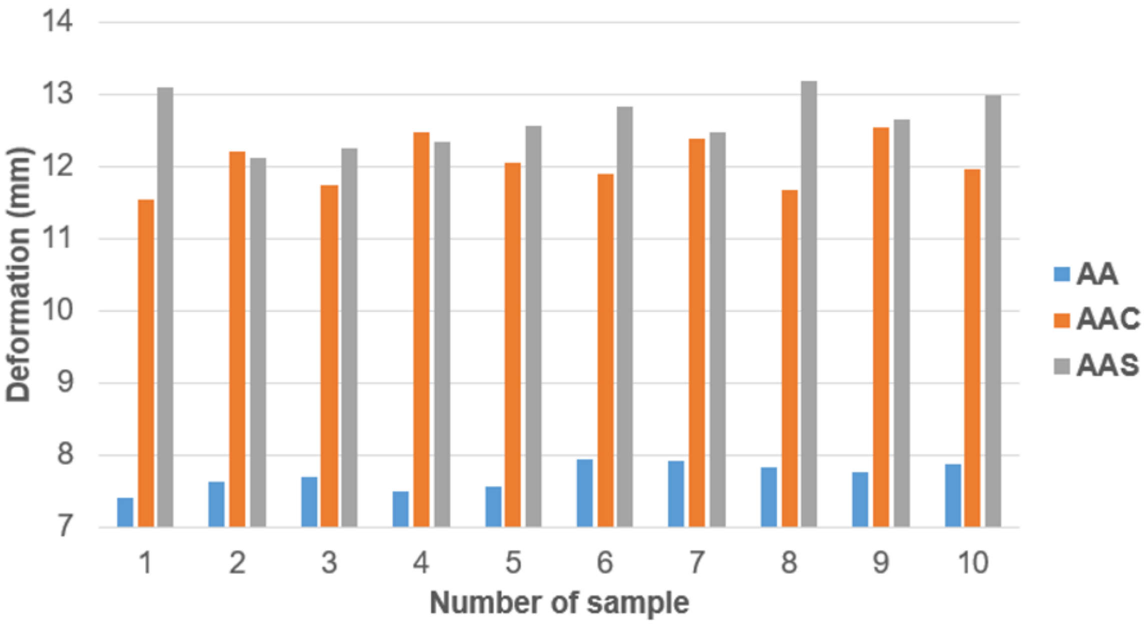

Fig. 8. Flexural deformation recorded for 10 specimens of each material group during the bending test

The absence of a statistically significant difference between AAC and AAS deformation values may be attributed to the similar global mechanical response of the cotton- and silk-reinforced composites under bending. Since both reinforcements had a bidirectional fiber distribution, the deformation behavior may have been governed more by the hybrid matrix and by the overall composite architecture than by the intrinsic differences between cotton and silk fibers. Possible interfacial effects, such as partial fiber–matrix debonding or local sliding, may also have contributed to this behavior; however, this remains only a hypothesis, as no dedicated interfacial or microscopic analysis was performed to confirm it.

The results demonstrate that reinforcement led to substantial improvements in bending behavior, with AAC exhibiting the highest flexural strength, while AAS showed the greatest deformation capacity. A possible explanation for this behavior lies in the intrinsic mechanical response of the reinforcing fibers. Cotton fibers tend to exhibit higher stiffness, which contributes to improved load-bearing capacity and increased flexural strength. In contrast, silk fibers allow larger deformations before failure, leading to enhanced displacement and ductility.

Vibration Test

For the vibration experiments, the specimens were securely clamped at one end using a vice fixed to a rigid support, ensuring stable boundary conditions during testing. Each specimen was analyzed with a free span of 180 mm. The damping behavior was evaluated using the logarithmic decrement approach (Mirițoiu *et al.* 2026). The obtained results are illustrated in Figs. 9 and 10.

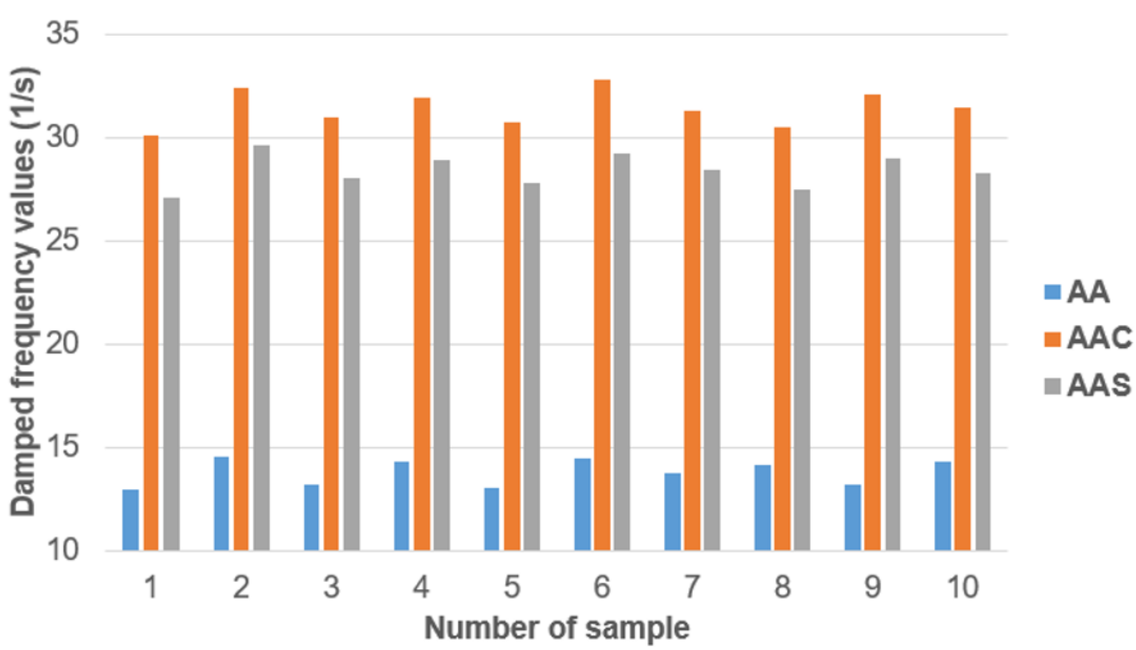

Fig. 9. Measured damped natural frequency for 10 samples within each material group

The recorded amplitude–time response was analyzed directly in the time domain, without using an FFT. The damping factor, μ, was calculated using the logarithmic decrement method presented in Eq. 1.

$$\mu = \frac{1}{t_2 - t_1} ln\left(\frac{v_1}{v_2}\right) \quad (1)$$

In Eq. 1, v_1 and v_2 are two selected maximum amplitudes recorded at times t_1 and t_2, respectively. The vibration frequency was calculated with Eq. 2. In Eq. 2, n is the number of complete oscillations occurring between t_1 and t_2.

$$\nu = \frac{n}{t_2 - t_1} \quad (2)$$

The vibration analysis highlights a significant influence of the reinforcement type on both damped natural frequency and damping behavior. The AAC specimens exhibited the highest damped natural frequency values, indicating increased stiffness and dynamic rigidity, while the AA specimens showed the lowest values. In contrast, the damping factor increased progressively from AA to AAS, with AAS presenting the highest energy dissipation capacity. A possible explanation for the observed behavior is related to the mechanical response of the reinforcing fibers. Cotton fibers tended to increase the overall stiffness of the composite, leading to higher natural frequencies. In contrast, silk fibers allowed greater internal deformation and energy dissipation during vibration, which resulted in increased damping capacity.

A statistical power analysis confirmed that testing 10 specimens per group ensured highly reliable results for both damped natural frequency and damping factor (power ≈ 1). No outliers were identified in the datasets, as indicated by the Dixon test ($\alpha = 0.05$). One-way ANOVA revealed a highly significant effect of the material configuration (AA, AAC, and AAS) on both damped natural frequency ($F = 1476.5$, $p = 10^{-18}$) and damping factor ($F = 377.3$, $p = 10^{-25}$).

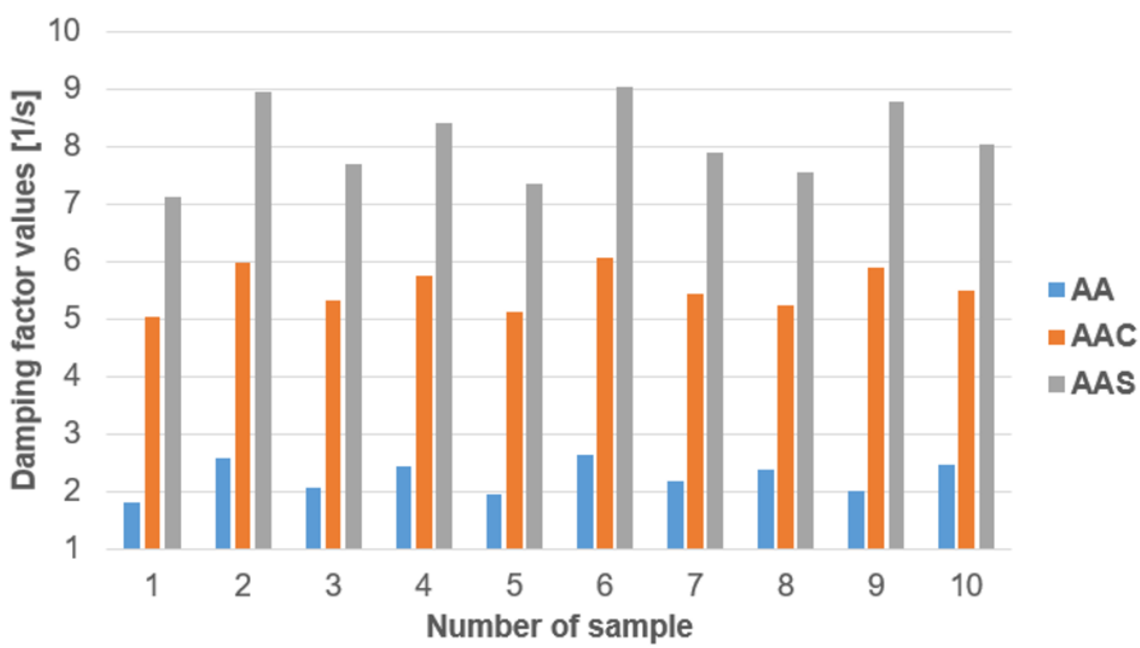

Fig. 10. Damping characteristics evaluated for a set of 10 specimens corresponding to each material type

Levene's test confirmed the homogeneity of variances for damped natural frequency ($p = 0.747$), while for the damping factor a deviation from variance homogeneity was observed ($p = 0.020$). The Shapiro–Wilk test yielded p-values of 0.113, 0.950, and

0.958 for damped natural frequency (AA, AAC, and AAS, respectively), and 0.503, 0.501, and 0.513 for the damping factor, confirming that the data followed a normal distribution. Therefore, a non-parametric Kruskal–Wallis test was additionally performed for the damping factor, confirming the statistical significance of the differences between groups ($p = 2.49 \cdot 10^{-6}$). Post hoc Bonferroni analysis ($\alpha = 0.0167$) demonstrated statistically significant differences between all material pairs. For damped natural frequency, the p-values were $1.58 \cdot 10^{-20}$ (AA vs AAC), $1.66 \cdot 10^{-19}$ (AA vs AAS), and $5.80 \cdot 10^{-7}$ (AAC vs AAS). For the damping factor, the corresponding adjusted p-values were $4.58 \cdot 10^{-14}$, $5.80 \cdot 10^{-15}$, and $1.41 \cdot 10^{-8}$.

Shore D Hardness Test

The final stage of the experimental program involved the evaluation of material hardness using the Shore D scale. Measurements were performed at 5 distinct locations distributed along the longitudinal symmetry axis of each specimen, and the resulting mean values are summarized in Fig. 11. Stiffness represents the ability of a material to resist deformation when subjected to external loading. A lower deformation under the same applied force corresponds to a higher stiffness level. In Shore hardness testing, this property is assessed by determining the penetration depth of a standardized indenter into the material surface, using a calibrated durometer. Materials with higher hardness exhibit greater resistance to indentation, as their internal structure more effectively opposes the applied load.

The Shore D hardness measurements revealed a clear influence of the material configuration on surface mechanical properties. The AAC specimens exhibited the highest hardness values, indicating a superior resistance to indentation and a more rigid surface behavior. The AAS samples showed intermediate hardness values, while the AA specimens presented the lowest hardness levels. This trend confirms that the introduction of reinforcement enhanced the resistance to localized deformation, with cotton-based reinforcement leading to the most pronounced increase in hardness.

A statistical power analysis confirmed that using 10 specimens per group ensured highly reliable Shore D hardness results (power = 1.000). No outliers were detected, as indicated by the Dixon test ($\alpha = 0.05$). One-way ANOVA revealed a highly significant effect of the material configuration (AA, AAC, and AAS) on hardness ($F = 689.416$, $p = 1.08 \cdot 10^{-16}$). Levene's test confirmed homogeneous variances ($p = 0.834$), while the Shapiro–Wilk test indicated normal data distribution for all groups, with p-values of 0.275, 0.624, and 0.553 for AA, AAC, and AAS, respectively. Bonferroni post hoc analysis ($\alpha = 0.0167$) showed significant differences between all material pairs (AA vs AAC: $p = 3.57 \cdot 10^{-18}$, AA vs AAS: $p = 2.04 \cdot 10^{-11}$, AAS vs AAC: $p = 1.36 \cdot 10^{-13}$). Overall, AAC exhibited the highest Shore D hardness, followed by AAS, while AA showed the lowest values, confirming that reinforcement increases resistance to indentation and material stiffness.

The present study was limited to the short-term mechanical, hardness, and free-vibration behavior of the investigated materials under laboratory ambient conditions. The effects of moisture absorption, cyclic humidity, temperature variations, thermal ageing, and prolonged environmental exposure were not evaluated. These factors may influence the dimensional stability, fiber–matrix interface, mechanical performance, and damping behavior of composites containing natural constituents. Future research will therefore investigate water absorption, environmental and thermal ageing, and the evolution of mechanical and dynamic properties after controlled exposure conditions. Further microstructural examination of the fiber–matrix interface will also be conducted to clarify the mechanisms governing the different responses of cotton- and silk-reinforced composites. These investigations will support the evaluation of *Abies alba*-modified composites for lightweight panels, furniture components, and non-load-bearing structural boards.

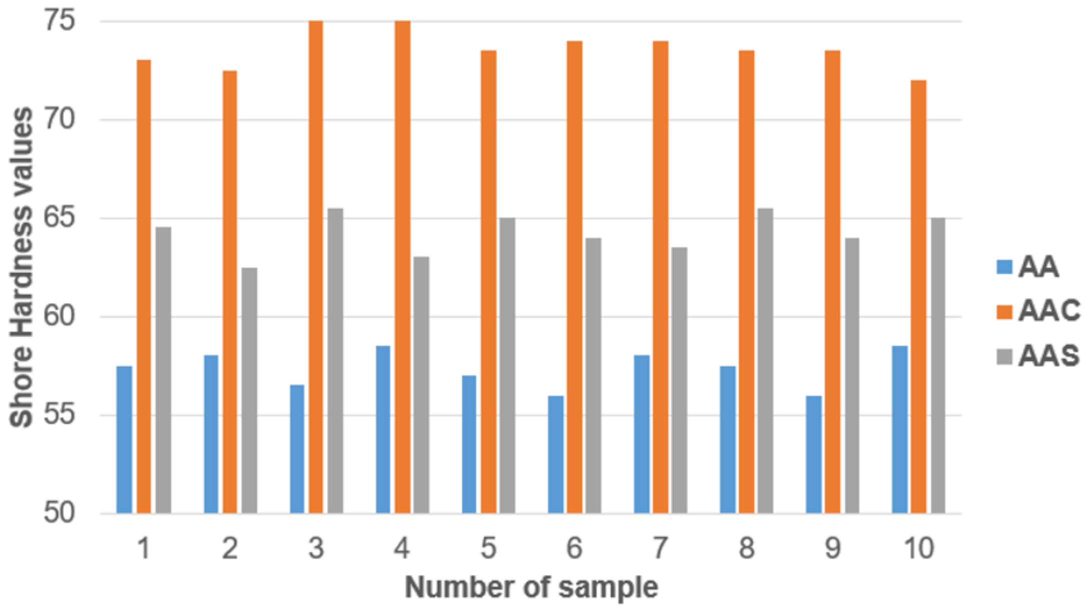

Fig. 11. Shore D hardness measured for 10 specimens in each material group

CONCLUSIONS

1. The introduction of textile reinforcement led to a significant improvement in all investigated mechanical properties compared to the unreinforced hybrid resin. Both cotton-reinforced (AAC) and silk-reinforced (AAS) composites exhibited superior tensile strength, flexural strength, stiffness, and hardness compared to the default specimens (AA) that contained just the 50:50 blend of *Abies alba* exudate and epoxy resin.
2. Cotton fiber reinforcement (AAC) resulted in the highest tensile and flexural strength, as well as the highest hardness values, indicating an increased load-bearing capacity and structural rigidity. In contrast, silk fiber reinforcement (AAS) led to higher deformation values and improved ductility, both under tensile and bending loading conditions.
3. The vibration analysis showed that AAC composites exhibited higher natural frequencies, indicating increased stiffness, while AAS composites demonstrated superior damping capacity, reflecting enhanced energy dissipation.
4. The statistical analysis (ANOVA with Bonferroni post hoc tests) confirmed that the material configuration had a highly significant influence on all investigated properties ($p < 0.05$). For most parameters, all material pairs exhibited statistically significant differences. An exception was observed in the case of flexural deformation, where no significant difference was found between AAC and AAS, suggesting a similar global deformation behavior under bending.

5. The absence of a statistically significant difference between AAC and AAS in flexural deformation can be attributed to the similar global mechanical response of the bidirectionally reinforced composites. In this case, the deformation behavior appeared to be governed more by the hybrid matrix and the overall composite architecture than by the intrinsic differences between cotton and silk fibers. Possible interfacial effects, such as partial fiber–matrix debonding or local sliding, may also contribute to this behavior; however, this remains a hypothesis that requires further investigation.
6. The results demonstrated that hybrid epoxy systems modified with *Abies alba* exudate can be successfully used as matrices for bio-based composites. The choice of reinforcement allows tailoring the mechanical response of the material, enabling a balance between strength (cotton reinforcement) and ductility/damping (silk reinforcement).

REFERENCES CITED

Ansari, M. F., Sarkhel, G., Goswami, D. N., and Baboo, B. (2014). "Coating properties of shellac modified with synthesised epoxidised-novolac resin," *Pigment & Resin Technology* 43(5), 314-322. https://doi.org/10.1108/PRT-06-2013-0111

ASTM D790-17 (2017). "Standard test methods for flexural properties of unreinforced and reinforced plastics and electrical insulating materials," ASTM International, West Conshohocken, PA, USA.

ASTM D2240-15 (2021). "Standard test method for rubber property—Durometer hardness," ASTM International, West Conshohocken, PA, USA.

ASTM D3039 (2014). "Standard test method for tensile properties of polymer matrix composite materials," ASTM International, West Conshohocken, PA, USA.

Bolcu, D., Stănescu, M. M., and Miriţoiu, C. M. (2022). "Some mechanical properties of composite materials with chopped wheat straw reinforcer and hybrid matrix," *Polymers* 14(15), article 3175. https://doi.org/10.3390/polym14153175

Brocas, A.-L., Llevot, A., Mantzaridis, C., Cendejas, G., Auvergne, R., Caillol, S., Carlotti, S., and Cramail, H. (2014). "Epoxidized rosin acids as co-precursors for epoxy resins," *Designed Monomers and Polymers* 17(3), 301-310. https://doi.org/10.1080/15685551.2013.840504

Deng, L., Wang, Z., Qu, B., Liu, Y., Qiu, W., and Qi, S. (2023). "A comparative study on the properties of rosin-based epoxy resins with different flexible chains," *Polymers* 15(21), article 4246. https://doi.org/10.3390/polym15214246

El-Ghazawy, R. A., El-Saeed, A. M., Al-Shafey, H. I., Abdul-Raheim, A.-R. M., and El-Sockary, M. A. (2015). "Rosin based epoxy coating: Synthesis, identification and characterization," *European Polymer Journal* 69, 403-415. https://doi.org/10.1016/j.eurpolymj.2015.06.025

Franz, M. H., Neda, I., Maftei, C. V., Ciucă, I., Bolcu, D., and Stănescu, M. M. (2021). "Studies of chemical and mechanical properties of hybrid composites based on natural resin dammar formulated by epoxy resin," *Polymer Bulletin* 78, 2427-2438. https://doi.org/10.1007/s00289-020-03221-4

Goswami, D. N., and Kumar, S. (1984). "Study on the curing of shellac with epoxy resins by dielectric measurements," *Die Angewandte Makromolekulare Chemie* 126, 145-152. https://doi.org/10.1002/APMC.1984.051260115

Huang, K., Zhang, J., Li, M., Xia, J., and Zhou, Y. (2013). "Exploration of the complementary properties of biobased epoxies derived from rosin diacid and dimer fatty acid for balanced performance," *Industrial Crops and Products* 49, 497-506. https://doi.org/10.1016/j.indcrop.2013.05.024

Kanehashi, S., Oyagi, H., Lu, R., and Miyakoshi, T. (2014). "Development of bio-based hybrid resin, from natural lacquer," *Progress in Organic Coatings* 77, 24-29. https://doi.org/10.1016/j.porgcoat.2013.07.013

Li, C., Liu, X., Zhu, J., Zhang, C., and Guo, J. (2013). "Synthesis, characterization of a rosin-based epoxy monomer and its comparison with a petroleum-based counterpart," *Journal of Macromolecular Science, Part A: Pure and Applied Chemistry* 50(3), 321-329. https://doi.org/10.1080/10601325.2013.755879

Liu, H., Wu, X., Liu, Y., Guo, Z., Ge, Q., and Sun, Z. (2022). "The curing characteristics and properties of bisphenol A epoxy resin/maleopimaric acid curing system," *Journal of Materials Research and Technology* 21, 1655-1665. https://doi.org/10.1016/j.jmrt.2022.10.008

Miritoiu, C. M., Stănescu, M. M., Bolcu, D., Jiga, G., Rădoi, A. I., and Tudose, D. I. (2021). "About the mechanical properties for a type of green composites with hybrid dammar/sandarac matrix and natural reinforcements," *Macromolecular Symposia* 395, article 2000305.

Miriţoiu, C. M., Roşca, A. S., and Stancuţ, A. (2026). "Influence of resin composition on the performance of composites reinforced with recovered paper and poultry feathers," *BioResources* 21(1), 808-838. https://doi.org/10.15376/biores.21.1.808-838

Miriţoiu, C. M., Pădeanu, P. A., and Cioateră, N. (2026). "Hybrid resins derived from *Abies alba* exudate as matrices for composite materials," *Polymers* 18(6), article 722. https://doi.org/10.3390/polym18060722

Obădan, M. E., Mitruţ, I., Ionescu, M., Obădan, F., Târtea, D. A., Popescu, M. A., Popescu, S. M., Smarandache, A. M., and Manolea, H. O. (2023). "Clinical efficacy analysis of the personalization of prosthetic abutments in implant-supported restorations in comparison to available standard titanium abutments," *Journal of Personalized Medicine* 13(9), article 1402. https://doi.org/10.3390/jpm13091402

Polydis (2023). "Polydis," (https://polydis.ro/), accessed 7 September 2023.

Popa, A. D., Vlăduţu, D. E., Turcu, A. A., Târtea, D. A., Ionescu, M., Păunescu, C., Stan, R. S., and Mercuţ, V. (2024). "Aspects of occlusal recordings performed with the T-Scan system and with the Medit intraoral scanner," *Diagnostics* 14(13), article 1457. https://doi.org/10.3390/diagnostics14131457

Takahisa, I., Rong, L., and Miyakoshi, T. (2006). "Studies on the reaction mechanism between urushiol and organic silane," *Progress in Organic Coatings* 55(1), 66-69. https://doi.org/10.1016/j.porgcoat.2005.10.003

Article submitted: May 6, 2026; Peer review completed: July 28, 2026; Revised version received and accepted: August 10, 2026; Published: August 26, 2026.
DOI: 10.15376/biores.21.4.10032-10048